Interpolative Background Subtraction

Michael L. Goris, Sharon G. Daspit, Peter McLaughlin, and Joseph P. Kriss

Stanford University Medical Center, Stanford, California

A method for background subtraction is presented. The data are digitized scintigraphic images, stored in 64 $\times$ 64 frames. Within this array a rectangular area surrounding the target is defined. All data points outside of this area are set equal to zero. From each data point within the area, the computer subtracts a background value equal to the average of the two intersecting linear interpolations between the values at the edges of the rectangular area having the ordinate and abscissa values of the point of interest. The rationale for this approach is discussed and its application in myocardial perfusion studies is illustrated.

J Nucl Med 17: 744–747, 1976

In a scintigraphic image, body or nontarget background is generally handled by subtraction across the board (threshold setting) or by delinearization of the display response (contrast enhancement). For some situations we have found it better to define background as a fixed fraction of the image area (*1*). In some cases, however, a more precise quantitation of the background is helpful. Schelbert et al. (*2*) and Van Dyck et al. (*3*) assumed that the count rate originating in the region adjacent to the target organ was representative of the background component of the target count rate. In effect, they used an average background, but the main thrust of their method was to take the background sample as a ring around the target. Both groups of investigators showed empirically that a left ventricular ejection fraction, calculated using this correction, agreed quite well with the value obtained by contrast ventriculography (area measurements). They also showed that although there is some predictability, there is enough variation to make several regional samplings (i.e., a ring) necessary.

We surmised that if the changes in regional background are relatively monotone, the background could be better approximated by linear interpolations than by simple averaging. An obvious application lies in the estimation of myocardial perfusion with ^{201}Tl-chloride, where one compares relative myocardial uptake of the tracer injected at rest and during exercise (*4*). This comparison is made difficult by the varying background component, which is usually larger in the resting study.

MATERIALS AND METHODS

Two millicuries of ^{201}Tl-chloride is injected intravenously with the patient at rest or exercising to angina or ST-segment changes on electrocardiography. Data are collected between 5 and 30 min in the anterior, left anterior oblique, and left lateral projections. The scintillation cameras are interfaced with a dedicated digital computer (*5*), and the scintigrams are digitized and stored as 64 $\times$ 64 data arrays [IA(K,L)].

Prior to background subtraction, the digitized images are smoothed by weighted nine-point averaging. The smoothed data are then displayed on a cathode-ray tube. On this display the operator selects two sets of coordinates (x_1, y_1) and (x_2, y_2) representing two opposite corners of a rectangle surrounding the target and whose sides parallel the coordinate axes, as do the rows and columns of the 64 $\times$ 64 data array forming the digitized image.

If IX1 = x_1, IY1 = y_1, IX2 = x_2, IY2 = y_2, then

Received Dec. 30, 1975; original accepted Feb. 3, 1976.

For reprints contact: M. L. Goris, Div. of Nuclear Medicine, Stanford University Medical Center, Stanford, CA 94305.

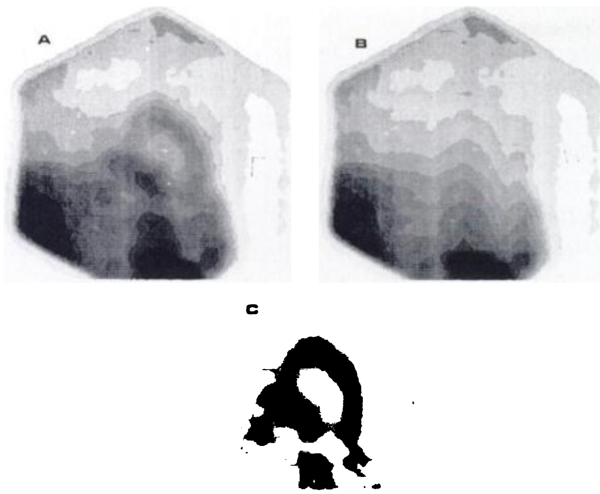

FIG. 1. Pseudograyshade display of count-rate distribution over chest (anterior view) after intravenous injection of 2 mCi of ^{201}Tl: (A) original data; (B) background computed by interpolation; and (C) residual, presumed to represent tracer distribution over myocardium. Note that inferior apical defect is better seen in residual image (C).

the picture elements IA(K,L) can be divided into three classes. The first class contains picture elements representing counts outside of the rectangular area, and whose x coordinates are smaller than x_1 (K < IX1) or larger than x_2 (K > IX2) and/or whose y coordinates are smaller than y_1 (L < IY1) or larger than y_2 (L > IY2). All the elements in this first class are given an initial value of zero. The second class contains elements representing counts within the rectangular area; their x coordinates lie between x_1 and x_2 and their y coordinates lie between y_1 and y_2 (IX1 < K < IX2, IY1 < L < IY2). For each such element the background component is computed as the average of two intersecting linearly interpolated values. The first interpolation is between the two points on the rectangle with the same x coordinate as the element in question, but with y coordinates equal to y_1 and y_2. The second interpolation is between two points with the same y coordinate as the element considered, but x coordinates x_1 and x_2.

Hence, the background at any point (K,L) is computed as

$$\mathrm{IBCK(K,L) = (IB1 + IB2)/2},$$

where

$$\mathrm{IB1 = IA(K,IY1) + [IA(K,IY2) - IA(K,IY1)]\frac{(L - IY1)}{(IY2 - IY1)}},$$

$$\mathrm{IB2 = IA(IX1,L) + [IA(IX2,L) - IA(IX1,L)]\frac{(K - IX1)}{(IX2 - IX1)}}.$$

The value IBCK(K,L) is then subtracted from the original corresponding IA(K,L) element.

The third and last class of picture elements consists of the edge elements delineating the selected rectangular area. (Either IX1 ≦ K ≦ IX2 and L = IY1 or IY2, or IY1 ≦ L ≦ IY2 and K = IX1 or IX2.) These elements are used as above to estimate the background component of the picture elements of the second class. In a final step the elements in the third class are set to zero. The digitized image, now smoothed and corrected for background, is plotted by an electrostatic printer–plotter, using a pseudogray scale display (*6*).

RESULTS AND DISCUSSION

Figures 1, 2, and 3 show data obtained in the anterior, left anterior oblique, and left lateral projections after an injection of 2 mCi of ^{201}Tl-chloride. The patient, a 28-year-old woman, had a history of recent anterior wall infarction, anterior wall aneurysm, and total obstruction of the left anterior descending coronary branch. The figures show the original smoothed data (A), the computed background (B), and the residual image (C). The myocardium is better delineated and the perfusion de-

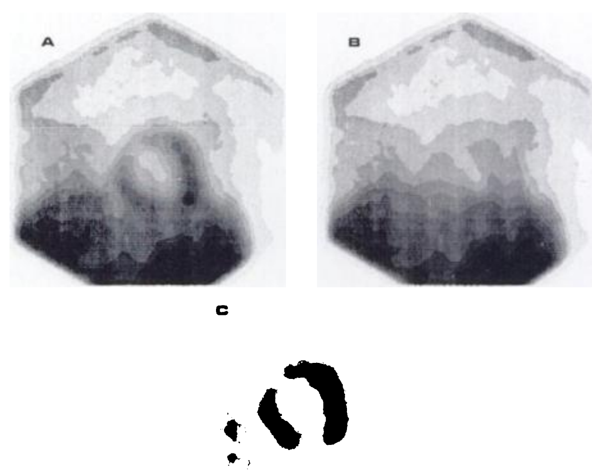

FIG. 2. Left anterior oblique view from same study: (A) original data; (B) interpolated background; and (C) residual. Again, inferior apical defect is better seen in residual image (C).

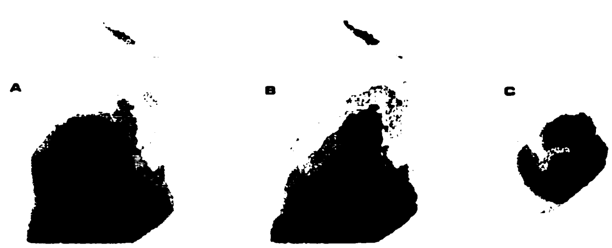

FIG. 3. Left lateral view from same study; (A) original data; (B) interpolated background; and (C) residual. Large anterior wall defect is seen in residual image, with suggestion of aneurysm.

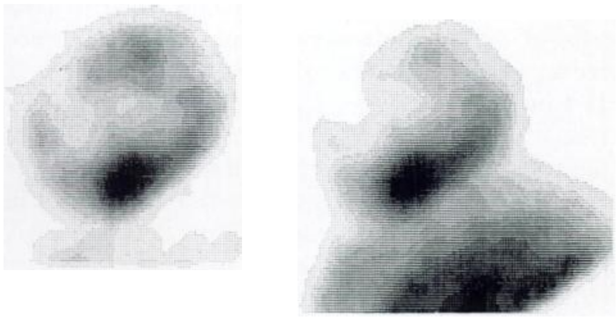

FIG. 4. Comparison of two background subtraction methods, using same data as in Fig. 3. (Left) I-terpolated background is subtracted; (right) constant average background is subtracted. Constant-background method oversubtracted from anterior wall and failed to remove subdiaphragmatic activity.

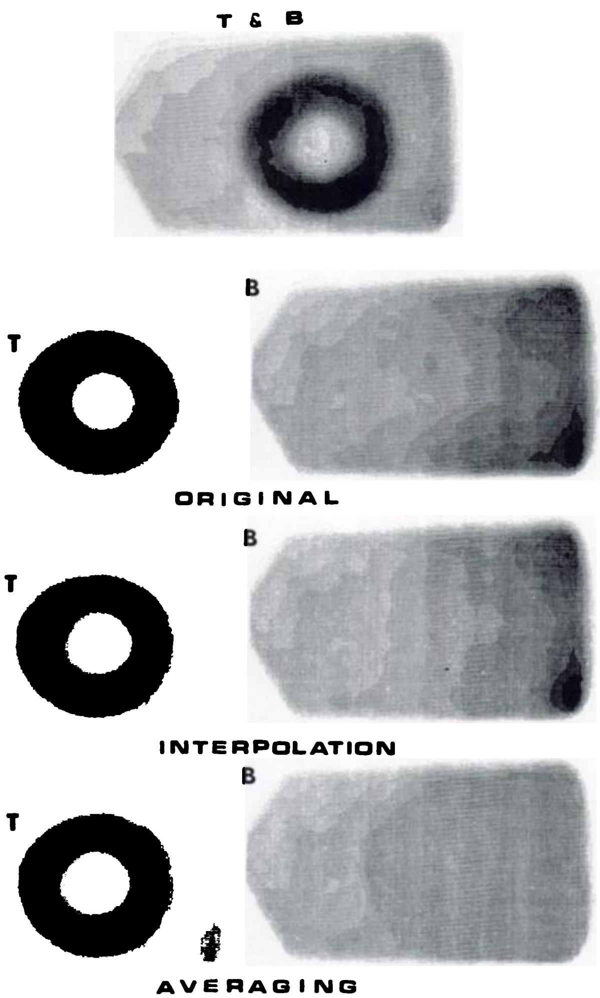

FIG. 5. Phantom on right contained progressively increasing activity and was used to simulate monotonely variable background. Second (smaller) phantom served as ring-shaped target, with slightly more activity on one side. Counts were collected separately for each phantom (second row) and then added (top). Third row shows residual obtained by interpolative subtraction. Fourth row shows result of subtracting constant average background.

fects in the apex, anterior wall, and proximal septum are more clearly seen in the corrected images (C). Although well-chosen contrast enhancement could have achieved the same effect, it is unreasonable to expect contrast enhancement alone to equalize the contrast between target and background obtained during exercise and rest without introducing other artifacts. On the other hand, the computed background (B) is what one would expect: variation in a fairly monotone fashion. It corresponds well to the background surmised and mentally subtracted by the experienced reader in his visual interpretation of the "A" images.

Figure 4 shows the same data as Fig. 3 processed in two different ways: after the interpolative background subtraction (left) and after conventional constant-background subtraction (right). In the latter, the subdiaphragmatic activity still shows. Figure 5 uses phantom data to make the same comparison. This figure illustrates three things: (A) if the background is indeed monotonely variable, then the interpolative method will yield nearly exact results; (B) visual correction for background may fail, as shown in the top image where the unequal activity distribution in a ring phantom cannot be detected; and (C) conventional background subtraction will produce artifacts.

In general, if the background contribution to the image is not constant, the subtraction of a constant average background will introduce artifacts. For instance, if two points in the target have true counts of $n_1 > n_2$, but background contributions $b_1 < b_2$ so that the image shows $(n_1 + b_1)$ and $(n_2 + b_2)$, subtracting the average background $(b_1 + b_2)/2$ will yield $n_1 + (b_1 - b_2)/2$, which is less than the true count, and $n_2 + (b_2 - b_1)/2$, which is greater.

CONCLUSION

For the conditions described (a variable but monotone background), theoretical considerations show that an interpolated background subtraction is preferable to an averaged background subtraction. This is easily illustrated with phantoms having the appropriate characteristics. In the clinical application of myocardial scintigraphy with thallium, the procedure was found to be helpful in the interpretation of the data.

ACKNOWLEDGMENT

This work was supported in part by a gift from the Henry J. Kaiser Family Foundation.

REFERENCES

1. Goris ML, Kriss JP: A method to optimise the use of a grayshade scale in nuclear medicine images. *Comput Biomed Res*: to be published

2. Schelbert HR, Verba JW, Johnson AD, et al.: Non-

traumatic determination of left ventricular ejection fraction by radionuclide angiocardiography. *Circulation* 51: 902–909, 1975

3. VAN DYKE D, ANGER HO, SULLIVAN RW, et al.: Cardiac evaluation from radioisotope dynamics. *J Nucl Med* 13: 585–592, 1972

4. BERMAN DS, SALEL AF, DENARDO GL, et al.: Noninvasive detection of regional myocardial ischemia using rubidium-81 and the scintillation camera. *Circulation* 52: 619–626, 1975

5. BUDINGER TF, HARPOOTLIAN J: Developments in digital computer implementation in nuclear medicine imaging. *Comput Biomed Res* 8: 26–52, 1975

6. GORIS ML, KRISS JP: Pseudogray shade hardcopy display of nuclear medicine data using a Versatec Matrix 1100A printer/plotter. In *Proceedings of Fifth Symposium on Sharing of Computer Programs and Technology in Nuclear Medicine, CONF-750124, Salt Lake City, Utah, 1975.* U.S. ERDA, 1975, pp 1–8

Accepted Articles To Appear in Upcoming Issues

In Vitro Stabilization of a Low-Tin Bone-Imaging Agent (^{99m}Tc-Sn-HEDP) by Ascorbic Acid. Accepted 1/22/76.
Andrew J. Tofe and Marion D. Francis

^{99m}Tc-Pyrophosphate Scan and Radiographic Correlation in Thyroid Acropachy (Case Report). Accepted 1/27/76.
Robert S. Seigel, James H. Thrall, and James C. Sisson

Scan Findings in a Case of Splenic Infarction Due to Amyloidosis (Case Report). Accepted 3/16/76.
Euishin Kim and Adel G. Mattar

Preparation of a Chemically Characterized ^{99m}Tc-Penicillamine Complex. Accepted 3/17/76.
Akira Yokoyama, Hideo Saji, Hisashi Tanaka, Teruo Odori, Rikushi Morita, Toru Mori, and Kanji Torizuka

Technetium-99m-Kethoxal-Bis(thiosemicarbazone), an Uncharged Complex with a Tetravalent Technetium State, and Its Excretion into the Bile. Accepted 3/17/76.
Akira Yokoyama, Yoshiaki Terauchi, Kazuko Horiuchi, Hisashi Tanaka, Teruo Odori, Rikushi Morita, Toru Mori, and Kanji Torizuka

Persistent Dural Cerebrospinal Fluid Leak Shown by Retrograde Radionuclide Myelography (Case Report). Accepted 3/18/76.
H. Kadrie, A. A. Driedger, and W. McInnis

Origin and Location of the Oral Activity in Sequential Salivary Gland Scintigraphy with ^{99m}Tc-Pertechnetate. Accepted 3/24/76.
H. P. van den Akker, E. Busemann Sokole, and J. B. van der Schoot

Digital Low-Pass Filtering. Accepted 3/29/76.
K. W. Buzzi, J. M. Weinraub, and G. A. L. Irwin

Rapid Determination of Oxidation State of Unbound ^{99m}Tc and Labeling Yield in ^{99m}Tc-Labeled Radiopharmaceuticals. Accepted 3/29/76.
Lelio G. Colombetti, Stephen Moerlien, Ghanshyam C. Patel, and Steven M. Pinsky

Liver-Spleen Scan in Sickle Cell Anemia (Letter to the Editor). Accepted 3/29/76.
A. M. Samuel, R. D. Ganatra, and P. Ramanathan

Splenic Accumulation of ^{99m}Tc-Diphosphonate (Letter to the Editor). Accepted 3/29/76.
Peter F. Winter

Lung Uptake of ^{99m}Tc-Sulfur Colloid in Falciparum Malaria (Case Report). Accepted 3/29/76.
Harvey A. Ziessman

Contamination with ^{131}I, ^{103}Ru, and ^{239}Np in the Eluate of ^{99}Mo-^{99m}Tc-Generators Loaded with (n,γ)-Produced ^{99}Mo. Accepted 4/1/76.
M. W. Billinghurst and F. W. Hreczuch

Acute Myocardial Infarction Imaged with ^{99m}Tc-Stannous Pyrophosphate and ^{201}Tl: A Clinical Evaluation. Accepted 4/2/76.
Robert W. Parkey, Frederick J. Bonte, Ernest M. Stokely, Samuel E. Lewis, Kenneth D. Graham, L. Maximilian Buja, and James T. Willerson

Value of Routine Cerebral Radionuclide Angiography in Pediatric Brain Imaging. Accepted 4/6/76.
Philip O. Alderson, David L. Gilday, Michelle Michael, and Arnold L. Wilkie

Radionuclide Bone-Scan Abnormalities in Leprosy (Case Report). Accepted 4/7/76.
Thomas G. Goergen, Donald Resnick, Anthony Lomonaco, and Charles W. O'Dell, Jr.

Tissue Distribution of ^{203}Pb-Acetate: Comparison with ^{67}Ga-Citrate as an Abscess-Localizing Agent. Accepted 4/13/76.
Andrew Taylor, Jr., Phillip Hagan, Naomi Alazraki, and Patricia Hall

Estimates of Radiation Dose to the Embryo from Nuclear Medicine Procedures. Accepted 4/15/76.
Edward M. Smith and G. G. Warner

Myocardial Localization of ^{99m}Tc-Pyrophosphate (Letter to the Editor). Accepted 4/16/76.
B. C. Lentle, F. I. Jackson, and J. R. Scott

Reply. Accepted 4/16/76.
Jagmeet S. Soin

Cost-Effectiveness of Lung Scanning (Letter to the Editor). Accepted 4/16/76.
Marvin Guter and Stanley J. Goldsmith

Reply. Accepted 4/16/76.
Barbara J. McNeil

Routine Renal Imaging after ^{99m}Tc-Glucoheptonate Brain Scans. Accepted 4/19/76.
Paul C. Kahn, Mrinal K. Dewanjee, and Susan S. Brown

Monitoring Rejecting Renal Grafts with ^{99m}Tc-Sulfur Colloid (Letter to the Editor). Accepted 4/19/76.
Erica A. George, Robert E. Henry, and Robert E. Donati

Reply. Accepted 4/19/76.
Mathis P. Frick, Marvin E. Goldberg, Richard L. Simmons, and Merle K. Loken

Iodine-125-Digoxin Radioimmunoassay: Comparison of Commercial Kits. Accepted 4/20/76.
Danielle J. Battaglia and Michael L. Cianci

Pleural Oligemia Seen in Bone Scanning (Letter to the Editor). Accepted 4/20/76.
Mary Hauser and Eugene Cornelius

The Rim Sign in Epidural Hematoma (Case Report). Accepted 4/20/76.
Albert Zilkha and Gerald A. L. Irwin

Right Atrial Myxoma Presenting as Nonresolving Pulmonary Emboli (Case Report). Accepted 4/22/76.
Lawrence R. Muroff and Philip M. Johnson

Scintigraphic Detection of Hepatic Metastases with ^{131}I-Labeled Steroid in Recurrent Adrenal Carcinoma (Case Report). Accepted 4/22/76.
K. Watanabe, I. Kamoi, C. Nakayama, I. Koga, and K. Matsuura

Quality Assurance for ^{99m}Tc-Sn-Pyrophosphate. Accepted 4/22/76.
Michael K. Elson and Tex B. Shafer

Intercomparison of Myocardial Imaging Agents: ^{201}Tl, ^{129}Cs, ^{43}K, and ^{81}Rb. Accepted 4/22/76.
Hiroshi Nishiyama, Vincent J. Sodd, Robert J. Adolph, Eugene L. Saenger, Jeannine T. Lewis, and Marjorie Gabel

Gonadal Radiation Dose and Its Genetic Significance in Radioiodine Therapy of Hyperthyroidism. Accepted 4/23/76.
James S. Robertson and Colum A. Gorman

Significance of Delayed ^{67}Ga Localization in the Kidneys. Accepted 4/27/76.
Bharath Kumar and R. Edward Coleman

Renal Localization of ^{67}Ga-Citrate in Renal Amyloidosis (Case Report). Accepted 4/27/76.
Carlos Bekerman and Mahendra I. Vyas

Gallium Imaging in Pulmonary Artery Sarcoma Mimicking Pulmonary Embolism (Case Report). Accepted 4/27/76.
Paul J. Myerson, Daniel A. Myerson, Richard Katz, and J. P. Lawson

Effect of Tin-Induced Enzymes on Pertechnetate Distribution (Letter to the Editor). Accepted 4/27/76.
H. S. Winchell

Summation Peaks in a Well Scintillation Counter (Letter to the Editor). Accepted 5/4/76.
A. M. Passalaqua and R. Chandra

Reply. Accepted 5/4/76.
F. R. Hudson, H. I. Glass, and S. L. Waters

Intense Myocardial Uptake of ^{99m}Tc-Diphosphonate in a Uremic Patient with Secondary Hyperparathyroidism and Pericarditis (Case Report). Accepted 5/7/76.
Warren R. Janowitz and Aldo N. Serafini

Effects of Iron on ^{67}Ga Uptake (Letter to the Editor). Accepted 5/9/76.
A. A. Driedger

Reply. Accepted 5/9/76.
Timothy Merz

"Owl Eye" Sign in Thyroid Nodule of Papillary Carcinoma (Case Report). Accepted 5/10/76.
Richard Ravel

Diagnosis of Epidural Hematoma by Brain Scan and Perfusion Study (Case Report). Accepted 5/10/76.
Daniel J. Buozas, Ivan R. Barrett, and Fred S. Mishkin

A New Dual-Probe System for the Rapid Bedside Assessment of Left Ventricular Function. Accepted 5/11/76.
Mark W. Groch, Stuart Gottlieb, Stephen M. Mallon, and August Miale, Jr.

Preparation of ^{99m}Tc-Labeled Red Blood Cells (Letter to the Editor). Accepted 5/11/76.
R. F. Gutkowski, H. J. Dworkin, W. C. Porter, and H. Rohwer

Reply. Accepted 5/11/76.
T. D. Smith and P. Richards

Affinity of Fibrin Deposits for ^{99m}Tc-Sulfur Colloid (Letter to the Editor). Accepted 5/11/76.
Milo M. Webber

A Simple Technique for Measuring Relative Renal Blood Flow. Accepted 5/13/76.
David M. Shames and Melvyn Korobkin

Right Ventricular Mean Transit Time (Letter to the Editor). Accepted 5/13/76.
Pierre P. Morin, Jean F. Morin, Jehan Caroff, and Armelle Savina

Reply. Accepted 5/13/76.
A. Dwyer, J. Wolberg, and G. Freedman